Electron states in curved quantum structures with varying radius

J. Gravesen

Department of Mathematics, Technical University of Denmark, DK-2800 Kgs. Lyngby, Denmark

M. Willatzen

Mads Clausen Institute for Product Innovation, University of Southern Denmark, DK-6400 Sønderborg, Denmark

Abstract

The influence of size and shape is investigated for quantum-dot electronic states and intra-band oscillator strengths adapting a method originally due to Stevenson. The present work solves the one-band envelope-function problem for conduction-band eigenstates in the framework of $\boldsymbol{k}\cdot\boldsymbol{p}$ theory using general curved coordinates. The eigenstates found are subsequently employed to express intra-band oscillator strengths and emphasis is given to the dependence of oscillator strengths on quantum-dot size and shape. We finally provide four simple examples.

Key words: quantum dots, electronic eigenstates, oscillator strengths, differential geometry
PACS: 73.21.La, 73.22.-f

1. Introduction

With recent advances in nanotechnology, it is now possible to grow almost any quantum-dot shape to nanometer accuracy. This calls for a better understanding on how to optimize quantum-dot properties by tailoring shape and size [2,3].

In this work, we focus on intra-band optical applications of quantum-dot structures and determine oscillator strengths in the framework of the $\boldsymbol{k}\cdot\boldsymbol{p}$ envelope-function approximation. This is done using a computationally effective method originally based on Stevenson's work for obtaining electromagnetic wave and acoustic solutions in waveguides of varying cross section [5,6].

Email addresses: j.gravesen@mat.dtu.dk (J. Gravesen), willatzen@mci.sdu.dk (M. Willatzen).

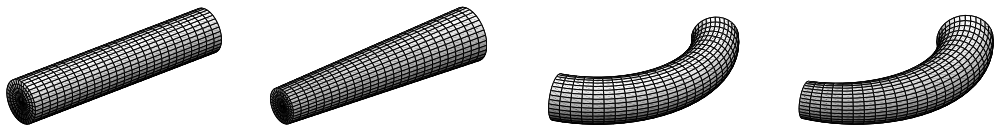

(a) (b) (c) (d)

Fig. 1. The length of the center curve is 20nm and the volume is $80\pi\text{nm}^3$ in all examples. Example a is the straight cylinder with radius 2nm. Example b is a truncated cone where the smallest and largest radius are in the proportion 1 : 2. Example c is a toroidal section where the center curve is part of a circle with radius 10nm. Example d has the same center curve as (c) and the same increasing cross sectional radius as (b).

The present work extends the method of Stevenson to account for curved structures of varying cross section. When cross-sectional dimensions are much smaller than the center-line dimension, the problem can be simplified to essentially a single ordinary differential equation. A full account of the procedure is in preparation [4].

The remaining part of this paper discusses the influence of size and shape of quantum-dot structures for intra-band optical oscillator strengths. Case examples are provided for the structures in Figure 1.

2. Stevenson's method

The nano-structures in Figure 1 can all be parametrized as a solid tube Ω around the center curve $\mathbf{r}$:

$$\mathbf{x}(s,\rho,\theta) = \mathbf{r}(s) + h(s)\rho(\cos\theta\,\mathbf{p}(s) + \sin\theta\,\mathbf{q}(s)), \tag{1}$$

where $(s,\rho,\theta) \in [0,L]\times[0,1]\times[0,2\pi]$, s is arc-length on the curve, $\mathbf{t}$ is the tangent vector of the curve, and $\mathbf{t},\mathbf{p},\mathbf{q}$ is a minimal rotating frame along the curve [1]. It is characterised by the equations $\mathrm{d}\mathbf{p}/\mathrm{d}s = -\kappa\cos T\,\mathbf{t}$ and $\mathrm{d}\mathbf{q}/\mathrm{d}s = -\kappa\sin T\,\mathbf{t}$ where κ is the curvature and $\mathrm{d}T/\mathrm{d}s = \tau$ is the torsion. The determinant of the metric tensor is $G = \rho^2F^2$, where $F = h^2(1-h\kappa\rho\cos(\theta+T))$. We observe that the L^2-norm on Ω is given by $\|\psi\|^2 = \int_0^L\int_0^{2\pi}\int_0^1 |\psi|^2\sqrt{G}\,\mathrm{d}\rho\,\mathrm{d}\theta\,\mathrm{d}s = \int_0^L\int_0^{2\pi}\int_0^1 |\sqrt{F}\psi|^2\rho\,\mathrm{d}\rho\,\mathrm{d}\theta\,\mathrm{d}s$ and that the map $\psi\mapsto\chi = \sqrt{F}\psi$ is an isometry between $L^2(\Omega)$ and $L^2([0,L]\times D)$, where D is the unit disk in $\mathbb{R}^2$. Helmholtz equation $\triangle\psi = E\psi$ in the tube Ω is equivalent to the eigenvalue problem $\sqrt{F}\triangle(\chi/\sqrt{F}) = E\chi$ in $L^2([0,L]\times D)$. Furthermore, $\langle\psi_1,\nabla\psi_2\rangle = \langle\chi_1,\sqrt{F}\nabla(\chi_2/\sqrt{F}\rangle$, where the inner products are in $L^2(\Omega)$ and $L^2([0,L]\times D)$, respectively.

Following Stevenson [5,6] we write $\chi\in L^2([0,L]\times D)$ as $\chi(s,\rho,\theta) = \sum_{k,\ell} c_{k,\ell}(s)\psi_{k,\ell}(\rho,\theta)$, where $\psi_{k,\ell}(\rho,\theta) = J_k(\lambda_{k,\ell}\rho)e^{ik\theta}$ are the eigenfunctions for the Laplace operator on the unit disk with Dirichlet boundary conditions. Here J_k is the k'th order Bessel function of the first kind and $\lambda_{k,\ell}$ is the ℓ'th zero of J_k. Substituting this into the eigenvalue problem $\sqrt{F}\triangle(\chi/\sqrt{F}) = E\chi$, written in s,ρ,θ coordinates, it is transformed into a system of coupled ordinary differential equations:

$$\sum_{k,\ell}\left(\alpha_{k,\ell;p,q}(s)\frac{\mathrm{d}^2}{\mathrm{d}s^2} + \beta_{k,\ell;p,q}(s)\frac{\mathrm{d}}{\mathrm{d}s} + \gamma_{k,\ell;p,q}(s)\right)c_{k,\ell} = \left(\frac{\lambda_{p,q}^2}{h^2} + E\right)c_{p,q}, \quad \text{all } p,q, \tag{2}$$

Table 1
The four lowest energies E_i for example a,b,c, and d in eV. To the left and in the middle calculated with one and four transversal modes respectively. To the right the L^2-norms of the higher transversal modes.

	E_1	E_2	E_3	E_4
a	0.866	0.998	1.218	1.526
b	0.814	1.037	1.277	1.583
c	0.865	0.998	1.220	1.529
d	0.814	1.037	1.279	1.587

	E_1	E_2	E_3	E_4
a	0.866	0.998	1.218	1.526
b	0.814	1.037	1.277	1.583
c	0.865	0.998	1.219	1.526
d	0.813	1.037	1.277	1.581

	1	2	3	4
a	0.000	0.000	0.000	0.000
b	0.001	0.001	0.002	0.003
c	0.003	0.012	0.029	0.057
d	0.010	0.024	0.046	0.092

where $\alpha_{k,\ell;p,q}$, $\beta_{k,\ell;p,q}$, and $\gamma_{k,\ell;p,q}$ are certain functions determined by the geometry of the structure Ω. By truncating the sum we obtain a finite system of ODE's, and for low energies only very few terms are needed.

Similar we have that the inner product $\langle \chi_1, F^{1/2}\nabla(F^{-1/2}\chi_2)\rangle$ can be written

$$\int_0^L \sum_{k,\ell,p,q} \Big(\big(\alpha_{\mathbf{t},p,q,k,\ell}(s) c_{1,p,q}(s) c'_{2,k,\ell}(s) + \beta_{\mathbf{t},p,q,k,\ell}(s) c_{1,p,q}(s) c_{2,k,\ell}(s)\big)\mathbf{t}(s) + \beta_{\mathbf{p},p,q,k,\ell}(s) c_{1,p,q}(s) c_{2,k,\ell}(s)\mathbf{p}(s) + \beta_{\mathbf{q},p,q,k,\ell}(s) c_{1,p,q}(s) c_{2,k,\ell}(s)\mathbf{q}(s)\Big)\, \mathrm{d}s, \quad (3)$$

where $\alpha_{\mathbf{t},p,q,k,\ell}$, $\beta_{\mathbf{t},p,q,k,\ell}$, $\beta_{\mathbf{p},p,q,k,\ell}$, and $\beta_{\mathbf{q},p,q,k,\ell}$ once more are functions determined by the geometry of the structure Ω.

3. Intra-band oscillator strengths

Intra-band oscillator strengths are in the one-band model approximation computed as: $\langle\psi_n|\boldsymbol{p}|\psi_m\rangle = \langle f_n|\boldsymbol{p}|f_m\rangle$, where $|\psi_n\rangle = f_n|S\uparrow\rangle$ for $|1/2, 1/2\rangle$ conduction-band electrons, etc., and f_n is the associated envelope function found by solving the problem in (2). It is well known that for parity-eigenstate envelope functions intra-band optical dipole elements are only nonzero between states of opposite parity (even-to-odd or odd-to-even envelope-function index transitions are allowed only). This will be the case if the geometry of the problem is inversion symmetric with respect to the quantum-dot center plane. In cases without inversion symmetry, intra-band oscillator strengths are generally nonzero for all transitions.

Envelope functions and associated energies are found by solving (2) subject to Dirichlet boundary conditions. The first four eigenstates are given in Table 1 for the four geometry examples: (a)-(d) in Figure 1 while the optical oscillator strengths for intra-band transitions between any two of the four states are listed in Table 2. Since the radius of the cylinder is much smaller than the length, envelope-function dependencies on the in-plane coordinates are the same for the first four eigenstates. Hence, oscillator strengths become zero for y or z-polarized light for the straight cylinder and straight truncated cone cases.

Evidently, due to lack of inversion symmetry for the quantum-dot structures in Figure 1b and d, optical oscillator strengths are now nonzero for intra-band transitions between any set of conduction-band states. Inversion symmetry is, however, preserved in Figure 1a and c and optical oscillator strengths become zero between states of similar parity.

Table 2
Optical oscillator strength in $\sqrt{\mathrm{eVm_0}}$. The entries in row k in the top tables are $\langle\psi_k|p_x|\psi_\ell\rangle$ for $k<\ell\leq 4$ for Example a–d. The entries in row k in the bottom tables to the left and in the middle are $\langle\psi_k|p_y|\psi_\ell\rangle$ for $k<\ell\leq 4$ for Example c and d. The entries in the bottom-right table are the maximal differences between optical oscillator strength when calculated with one and four transversal modes respectively.

a		
0.031i	0	0.012i
	0.056i	0
		0.080i

b		
0.038i	-0.019i	0.015i
	0.055i	-0.019i
		0.078i

c		
0.030i	0	0.007i
	0.052i	0
		0.073i

d		
0.036i	-0.016i	0.009i
	0.052i	-0.018i
		0.072i

c		
0	-0.017i	0
	0	-0.030i
		0

d		
0.008i	-0.017i	0.012i
	0	-0.026i
		-0.004i

	a	b	c	d
x	2.19e-09	5.86e-06	1.87e-03	2.56e-03
y	2.07e-16	1.22e-16	4.52e-04	2.72e-03
z	2.07e-16	1.22e-16	1.59e-16	3.63e-03

The curved structures have nonzero oscillator strengths for y-polarized light as expected given the fact that the centerline in Figure 1c and d is in the $x-y$ plane and not aligned with the x axis.

We emphasize that for the first four states, energies and optical oscillator strengths are well captured by a single mode as is revealed by Table 1 (right) and Table 2 (bottom-right). Hence, our calculations confirm that even for structures with complex geometry, a single ordinary differential equation suffices for the determination of 3D lower-lying quantum-dot states.

4. Conclusions

Quantum-dot conduction band eigenstates are found employing a model originally due to Stevenson for electromagnetic and acoustic waves but extended so as to account for general curved coordinates. The model output (envelope functions and energy eigenvalues) are finally used to compute intra-band optical transition strengths and emphasis is given to the influence of size and shape on allowed/forbidden transitions and their strengths. It is also shown that for low energies and cross-sectional dimensions much smaller than the quantum-dot centerline length, the extended Stevenson method on a (three dimensional) quantum-dot problem can be reduced, with good accuracy, to a single ordinary differential equation in the centerline coordinate.

References

[1] R. L. Bishop, *Amer. Math. Monthly,* **82**, 246 (1975).

[2] J. Gravesen, M. Willatzen, and L.C. Lew Yan Voon, J. Math. Phys., 46, 012107 (2005).

[3] J. Gravesen and M. Willatzen, Physical Review A 72, 032108 (2005).

[4] J. Gravesen and M. Willatzen, in preparation.

[5] A.F. Stevenson, J. Appl. Phys., **22**, 1447 (1951).

[6] A.F. Stevenson, J. Appl. Phys., **22**, 1461 (1951).